20th International Conference on Structural Mechanics in Reactor Technology (SMiRT 20)
Espoo, Finland, August 9-14, 2009
SMiRT 20-Division I, Paper 3142

Effect of hardening model on the weld residual stress field in pipe girth welds

Jonathan G. Mullins[1] and Jens Gunnars[1]

[1]Inspecta Technology AB, Lindhagensterrassen 1, Stockholm, Sweden,
e-mail: jonathan.mullins@inspecta.com, jens.gunnars@inspecta.com

Keywords: Weld residual stress, stainless steel, strain hardening.

1 ABSTRACT

Accurate estimates of weld residual stress fields in welded components are necessary for conducting structural assessments where stress corrosion cracking and/or fatigue are of interest. The aim of the study is to determine whether finite element simulations of the weld residual stress field give the best agreement with experimental measurements if an isotropic, kinematic or mixed material hardening model is used. Two girth weld geometries are considered with thicknesses of 19mm and 65mm and radius to thickness ratios of 10.5 and 2.8, respectively.

Welding simulations were conducted using isotropic, kinematic and mixed hardening models. The isotropic hardening model gave the best overall agreement with experimental measurements. The mixed hardening model gave good agreement for predictions of the hoop stress but tended to under predict the magnitude of the axial stress. The kinematic hardening model consistently under predicted the magnitude of both the axial and hoop stress. Although the conclusions need to be confirmed by further simulations and measurements for other geometries, an isotropic hardening model is recommended as the current best alternative for use in welding simulations.

2 INTRODUCTION

Detailed knowledge of the residual stress fields that result from welding processes is critical to performing damage tolerance analyses of nuclear structures. The through-thickness distribution of these weld residual stress fields influences the growth of cracks where either stress corrosion cracking or fatigue is of interest. This distribution is sensitive to geometry, material and welding parameters and must be accurately predicted in order to reach safe conclusions about structural integrity. For this reason considerable effort has been devoted to quantifying weld residual stress fields both experimentally and numerically. This report is based upon work sponsored by the Swedish Radiation Safety Authority (SSM) to verify and improve the weld residual stress modelling procedures currently used in Sweden. The focus of the present study is material hardening models.

In the past, welding simulation has been conducted using a kinematic hardening model but with recent developments in the area there has been a shift to the use of isotropic and even mixed hardening models. From the literature it is unclear which hardening model is best or even whether there is a significant difference in the residual stress fields obtained. In a recent project (Zang, 2008) an isotropic model provided a better agreement to experimental data for a range of girth weld geometries as compared to a kinematic model. Conversely recently published results from another study (Ogawa, 2008) indicated that the choice of hardening model did not have a significant influence on the weld residual stress field.

In this work we attempt to identify the effect that different hardening definitions can have on weld residual stress distributions and therefore rationalise the two apparently contradictory findings cited above. Three different hardening models are considered, for two girth weld geometries:

1. Isotropic, where flow curves at different temperatures are fully defined in tabular form.
2. Kinematic where the bilinear, “Ziegler”, implementation is used with a saturation strain of 0.1.
3. Mixed isotropic and kinematic “Lemaitre-Chaboche” hardening with fully defined, nonlinear isotropic and kinematic hardening definitions.

3 RESIDUAL STRESS MODELLING PROCEDURE

The procedure used in this work involves an initial transient thermal analysis of the welding process, followed by a mechanical analysis in order to determine deformations and residual stress fields.

3.1 Transient thermal analysis

The weld residual stress modelling procedure started with a transient thermal analysis of the welding heat flow. The transient thermal history provided input for a subsequent incremental thermo-elastic-plastic analysis and the thermal material properties used were temperature-dependent. A heat transfer boundary condition was applied at all free surfaces of the component and the boundary condition was altered in space as new weld passes were added. The heat source model was adapted to accommodate 2D axisymmetric simulations of the welding process; as described in detail by Zang (2008).

3.2 Thermo-elastic-plastic mechanical analysis

Once the temperature history was generated using the procedure described above, stresses and strains were calculated by performing a thermo-elastic-plastic analysis. The analysis follows the given temperature history on a pass per pass basis, until all weld passes have been simulated.

The mechanical properties were temperature-dependent and incremental plasticity was used. Parent and weld material were assigned the same material properties; details regarding the material hardening laws used may be found in Section 4. The multi-pass welds were modelled by activating the elements belonging to the current pass at a proper time, consistent with the transient heat flow simulation procedure. Strain relaxation for material that remelts was simulated using the new annealing capability in ABAQUS. The anneal temperature can simulate rapid strain relaxation at high temperatures, or in re-melted material. Data for the rate of recrystallization or creep at high temperatures is however rare, but recently published data (Lindgren, 2008) promotes an argument for a high anneal temperature – greater than 1300ºC.

Boundary conditions resembling the fixing conditions used during welding are applied to the model.

4 MATERIAL PROPERTIES AND HARDENING MODELS

4.1 Sources of data for plastic deformation of 316 stainless steel

For welding simulations it is important to use an accurate description of the material properties over temperature ranges from room temperature to the melting point (in this case approximately 1400^{o} Celsius). The thermal properties and the coefficient of thermal expansion for 316 stainless steel were taken from the report by Zang (2008). A traditional source of mechanical material data for 316 stainless steel is the standard ASME 240 (2004) but for welding simulations these minimum specified mechanical properties are not recommended, since they will lead to an underestimate of the magnitude of weld residual stresses. Instead other "best estimate" sources of data are needed. For isotropic and kinematic hardening models, the yield stress and the strain hardening properties must be specified up to, and exceeding a true plastic strain of approximately 0.15. For mixed kinematic hardening models cyclic stress strain curves are required for relevant strain ranges. A number of sources of mechanical data for 316 stainless steel were identified:

1. Sandmeyer steel company (2009) specified the yield stress and ultimate tensile stress of 316 stainless steel for temperatures ranging between 20 and 871ºC.
2. Albertini et al (1983) published flow curves for 316H stainless steel at strain rates between 10^{-3} and $10\ s^{-1}$ for temperatures of 20, 400 and 550ºC.
3. Lindgren et al (2008) published flow curves for 316L stainless steel at strain rates between $5x10^{-3}$ and $10s^{-1}$ for temperatures between 20 and 1300ºC.
4. Van Eeten (2005) published cyclic stress strain data for 316L stainless steel for a range of strain ranges at room temperature.
5. Ohmi et al (1995a, 1995b) published cyclic stress strain curves for 316 stainless steel for temperatures ranging between 20 and 700ºC.
6. Leggatt et al (2008) published parameters for a mixed hardening model for both 316L and 316H stainless steel for temperatures between 20 and 1400ºC.

There was no single source that could be used to fully define all the models in this study. Instead two data sources were chosen. Data for the isotropic and kinematic hardening models were taken from Lindgren et al (2008) since the yield stress, monotonic strain hardening response and strain rate sensitivity were fully

defined for the temperature range of interest. This is both the most recently published and most complete source of monotonic stress-strain curves for 316 stainless steel available in the literature. Data for the mixed hardening model was taken from Leggatt et al (2008) since a full set of mixed hardening parameters was available for the temperature range of interest.

4.2 Models for material hardening

4.2.1 Isotropic

With isotropic hardening the yield surface expands with accumulated plastic strain. In the implementation used here plastic incompressibility, initial isotropy, isotropic hardening and the normality rule are defined. Yielding occurs when

$$f = \sigma_{eq} - H - \sigma_y = 0 \tag{1}$$

where σ_{eq} is the von Mises equivalent stress, σ_y is the initial yield stress and H is the degree of strain hardening. Tabulated values of the flow stress are used to define H and the flow curves are reproduced in Figure 1. The strain rate at which the flow curves were taken was $10^{-2}s^{-1}$: inspection of welding simulation results reveals that this is a reasonable average estimate of the strain rate during a welding process. Note that the material displays a negative temperature sensitivity of the flow stress at temperatures between 600 and 700 ºC. This is consistent with dynamic strain aging (DSA) which has been observed to occur in 316 stainless steel in the past (Lindgren, 2008). Further, although it is difficult to discern from the chart, the material still strain hardens at 1300ºC which implies that it is appropriate to set the annealing temperature greater than this temperature. As discussed in section 3, in this study it was set to 1400ºC.

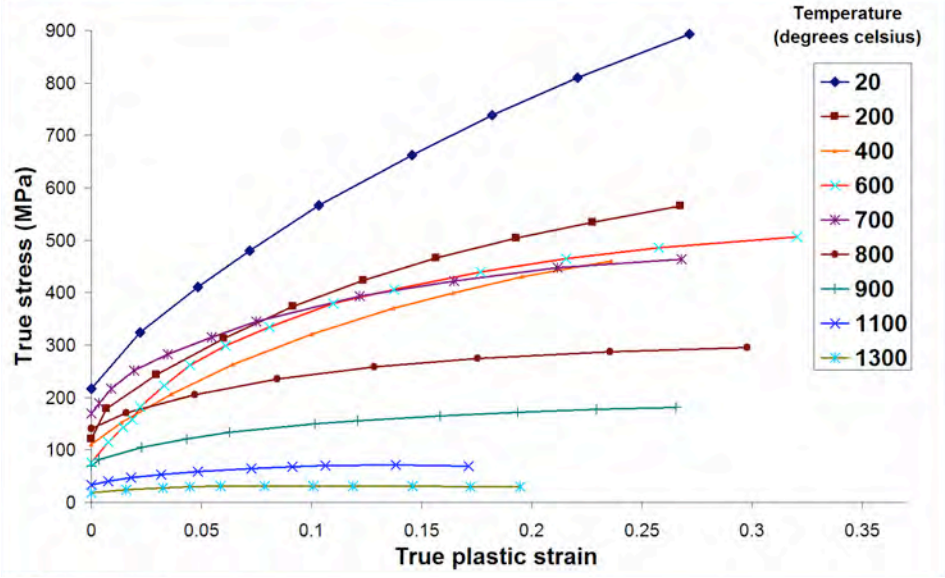

Figure 1. The flow stress of 316L stainless steel at a strain rate of $10^{-2}s^{-1}$ for temperatures between 20 and 1300ºC (Lindgren, 2008).

4.2.2 Kinematic

With kinematic hardening the concept of a backstress is introduced and the yield surface translates with accumulated plastic strain. In this study linear kinematic (Ziegler) hardening was used because it is available as a model within the ABAQUS material library. In this model the yield surface is defined by,

$$f = f(\sigma - X) - \sigma_y = 0 \tag{2}$$

where X is a backstress tensor whose rate of change is defined by,

$$\dot{X} = C\frac{1}{\sigma_y}(\sigma - X)\dot{\varepsilon}^{pl} \quad where\ 0 \le \varepsilon^{pl} \le \varepsilon_0, \text{ and}$$

$$\dot{X} = 0 \qquad where\ \varepsilon^{pl} > \varepsilon_0 \tag{3}$$

C is a material parameter and the saturation strain was set to equal 0.1. The data used to define $\dot{X}$ is available in (Mullins, 2009).

4.2.3 Mixed isotropic and kinematic

Mixed hardening was defined as per the nonlinear isotropic/kinematic hardening model available in ABAQUS. This model allows both expansion and translation of the yield surface. Here the yield surface is defined by Eqn (2). The isotropic and kinematic hardening components σ_y and $\dot{X}$ are, however redefined,

$$\dot{X} = C\frac{1}{\sigma_y}(\sigma - X)\dot{\varepsilon}^{pl} - \gamma X\dot{\varepsilon}^{pl}, \text{ and} \tag{4}$$

$$\sigma_y = \sigma_{y,0} + Q_\infty(1 - e^{-b\varepsilon^{pl}}) \tag{5}$$

γ and *b* are additional material parameters and $\sigma_{y,0}$ is the initial yield stress. The data used to define mixed hardening for 316H stainless steel was taken from (Leggat, 2008).

5 SIMULATIONS AND VALIDATION TO MEASURED RESULTS

The weld residual stress modelling procedure described in Section 3 was applied to two cases (see Table 1) where experimental residual stress measurements were available from the literature for well documented weld mock-ups. The purpose was to compare the weld residual stress predictions from different hardening models with experimental measurements. Three different analyses were conducted, where different hardening behaviours were specified:

- Isotropic with a fully defined flow curve using data for 316 published by Lindgren et al (2008).
- Linear kinematic with a saturation strain of 0.1 using data for 316 published by Lindgren et al (2008).
- Mixed, as specified by Leggat et al (2008) for 316H stainless steel.

Axi-symmetric modelling was used in all cases. The welding inter-pass temperature was assumed to be room temperature, which will tend to over-estimate residual stresses if the actual in-pass temperature were higher. The annealing temperature was set to 1400 °C.

The residual stress profiles have been measured in detail for these cases by neutron diffraction, deep-hole-drilling, and surface-hole drilling techniques, and documentation of the cases are found in (Bouchard, 2007; Edwards, 2000; Bate, 2000).

Table 1: Case definition.

Case No.	Name	Pipe thickness *t* [mm]	Pipe radius to thickness ratio R_{in}/t	Groove type	Number of passes	Weld type	Heat input [kJ/mm]	Material (parent/ weld)	Repair weld depth [mm]
1	SP19	19	10.5	V	14 (*)	MMA	1.35	316H/316L	~
2	S5VOR	65	2.8	V	45	MMA	2.4	316H/316L	~

(*) Data not fully clear from the mock-up manufacturing information available.

Measurements will always give an average value of the stress in a gauge volume in the material, and with some uncertainty with respect to the distance from the fusion line, see for example Price (2008). Considering this, care must be taken when choosing evaluation paths from finite element models. In the present study these evaluation paths were chosen to lie along the centre of the gauge volume. Stress distributions obtained in this way are suitable for comparison with experimental results provided the stress gradient perpendicular to the gauge volume is linear or nearly linear. This evaluation method was judged to be suitable for the present case. The measurement data used for comparison in Figures 6 and 7 were taken from an actual weld mock up and reflect measurements along a given path from the actual three dimensional pipe. As discussed by Dong (2001), the residual stress field in a multi-pass pipe butt-weld could have a periodic variation around the pipe circumference, in part connected with start and stop effects. This variation must be kept in mind when comparing experimental and numerically calculated weld residual stress fields.

5.1 Case 1 – Intermediate pipe

In the first case a medium thick-walled pipe having R_{in}/t = 10.5 was analysed. The geometry and the sequence of the weld passes is shown in Figure 2. Two through-wall paths are shown in Figure 2 – Path 1 was chosen for eventual comparison with experimental results. The pipe geometry is given in Table 1. Detailed information on the weld mock-up fabrication and welding process parameters were taken from (Bouchard, 2007; Edwards, 2000; Bouchard, 2005).

The finite element mesh and the peak temperature experienced during welding is shown in Figure 3. The fusion zone for the 14-pass weld is indicated by a temperature level exceeding 1400 °C. The HAZ is indicated by the temperature band ranging from 750 °C to the fusion line (1400 °C).

The predicted axial and hoop residual stress distributions, for the isotropic hardening model are shown in Figues 4 and 5. From Figure 5 it is seen that the stress field is asymmetrical around the weld centreline. This can be attributed to the welding sequence, most significantly the fact that the capping passes were applied from left to right.

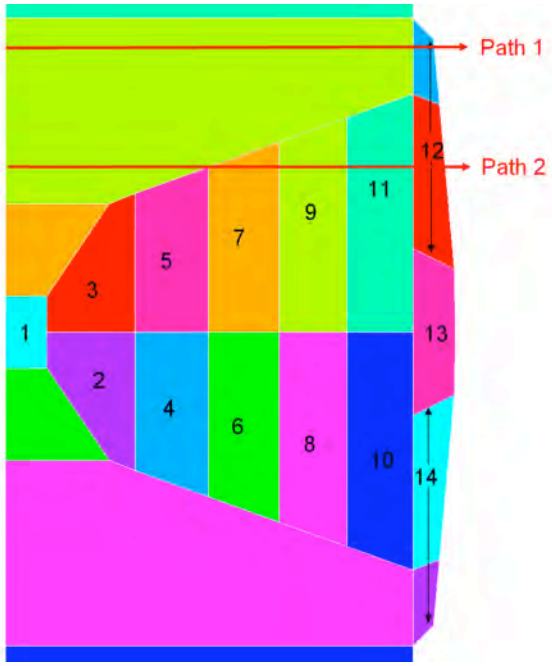

Figure 2: Geometry and definition of sequence of welding for Case 1.

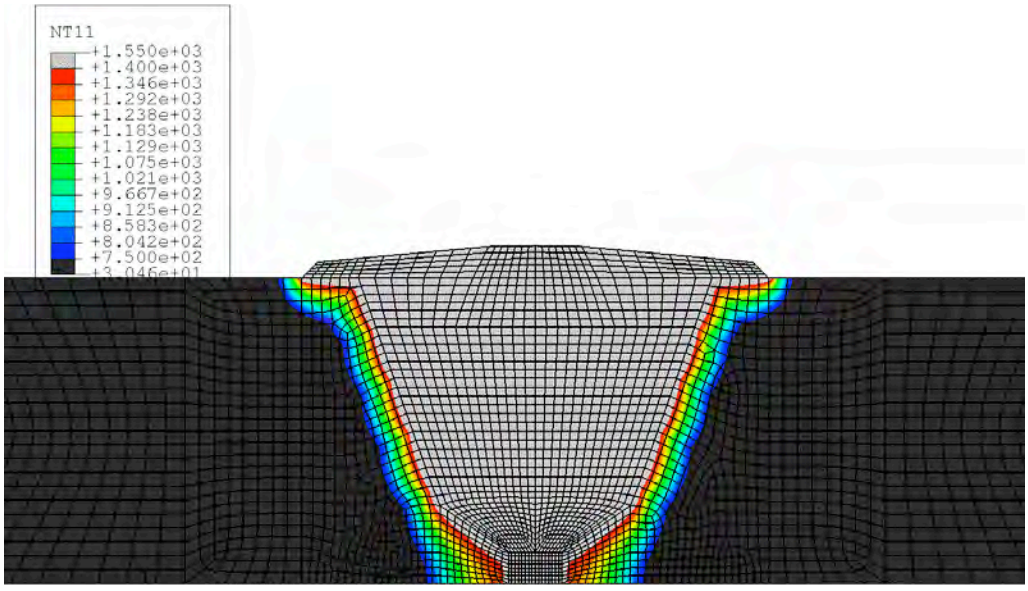

Figure 3: Fusion zone and HAZ. Maximum temperature experienced during the welding. The locations with maximum temperature >1400 °C are in gray, <750 °C are in black.

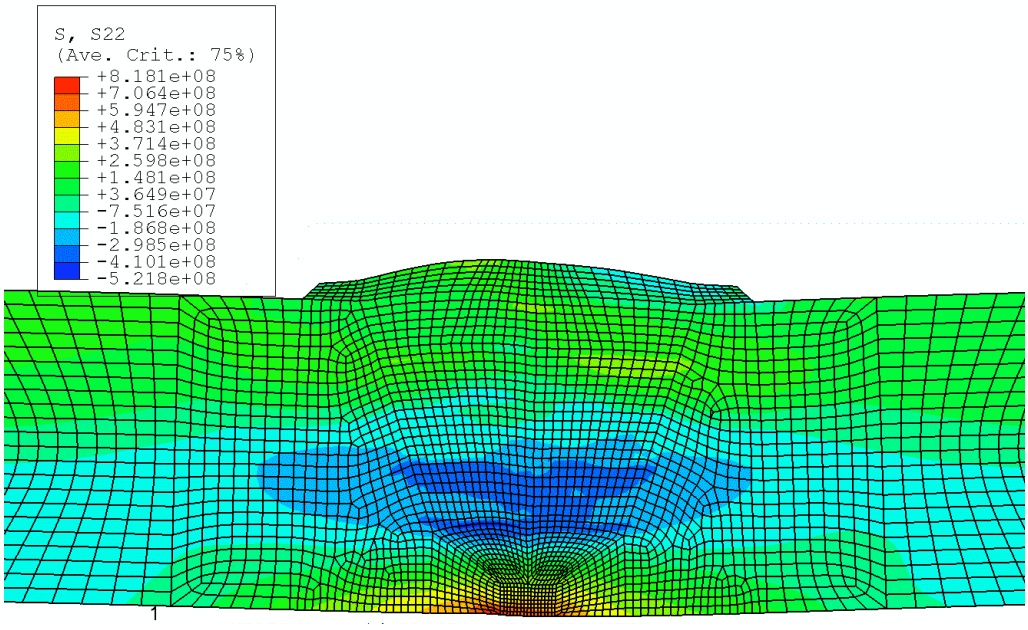

Figure 4: Axial residual stress for the medium thick-walled case 2 weld at 20 °C (unit Pa).

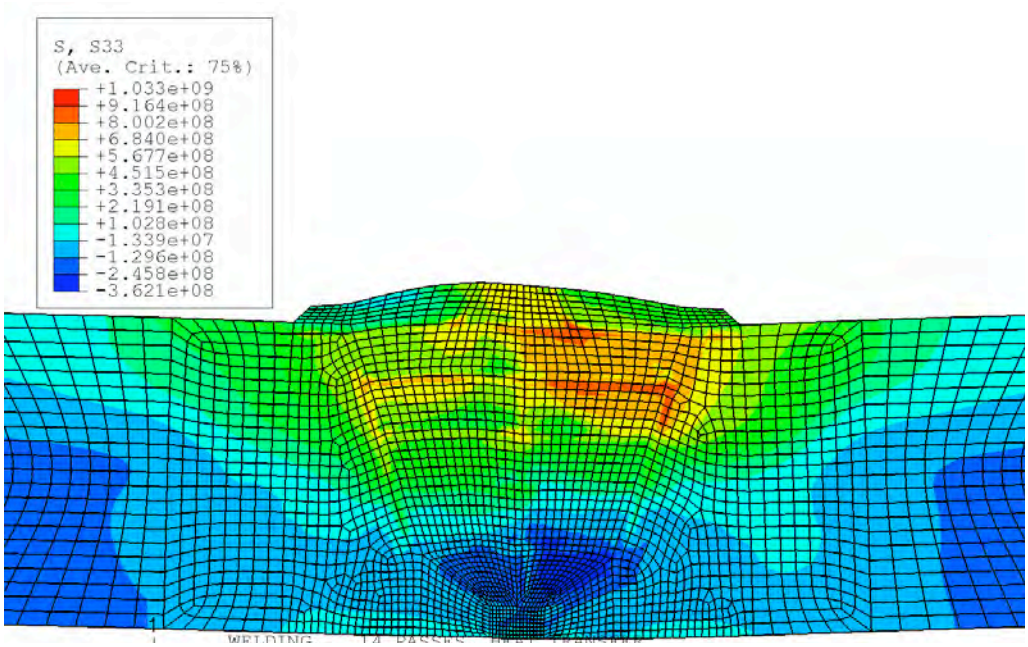

Figure 5: Hoop residual stress for the medium thick-walled case 2 weld at 20 °C (unit Pa).

The predicted residual stress distributions along Path1, as indicated in Figure 2, are compared with neutron diffraction measurements documented in (Bouchard, 2007; Edwards, 2000), as shown in Figures 6 and 7. This path lay mostly outside of the weld zone in parent metal, except towards the outer surface of the pipe, where it came into contact with the weld cap. The three modelling results shown correspond to the kinematic, isotropic and mixed hardening models. Best agreement is observed for the isotropic hardening model – where for the axial stress good agreement is observed for both the shape and the magnitude of the residual stress distributions. For the hoop stress good agreement is also obtained, except on the inner surface of the pipe where the stress magnitude is underestimated. With the kinematic hardening model the magnitude of the stress peaks was greatly underestimated for both the axial and the hoop stress. The distribution for the mixed hardening model lay between the isotropic and kinematic cases.

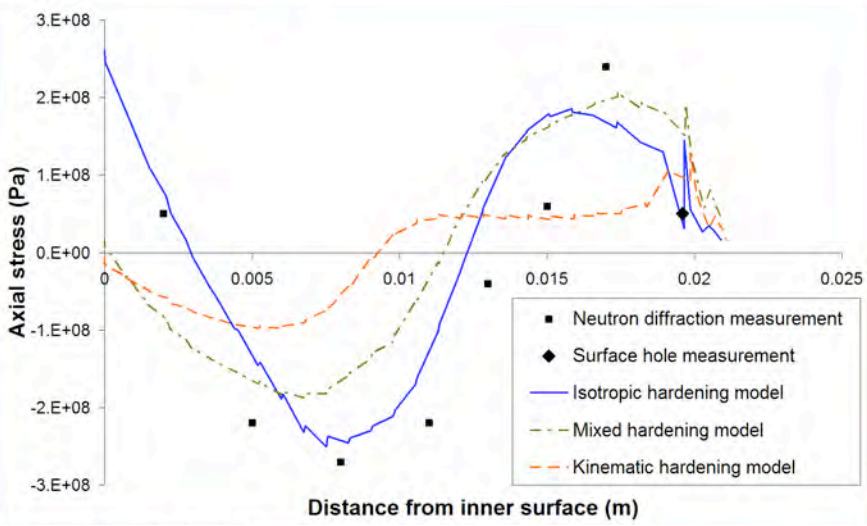

Figure 6: Case 1. Comparison of predicted axial residual stress along Path 1 (defined in Figure 2) for different hardening models. Available experimental data is also plotted.

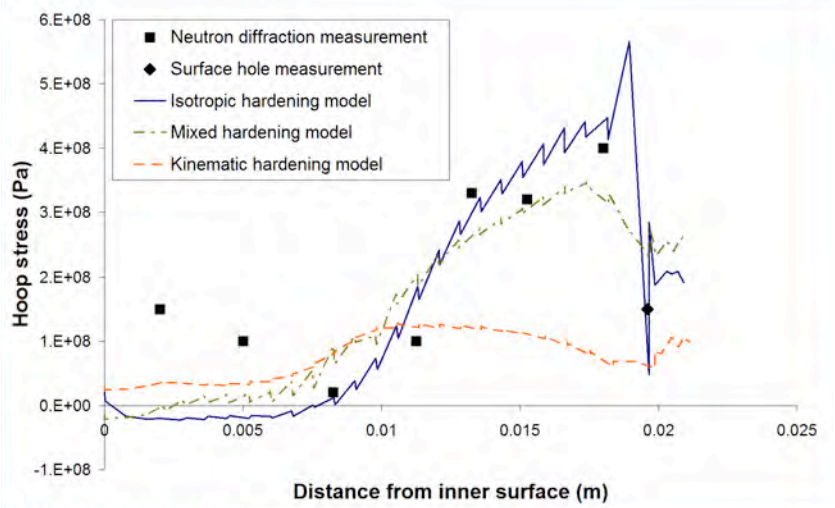

Figure 7: Case 1. Comparison of predicted hoop residual stress along Path 1 for different hardening models. Available experimental data is also plotted.

5.2 Case 2 – Thick-walled pipe

In case 2 a thick-walled pipe case having R_{in}/t = 2.8 was analysed. The geometry and the finite element mesh are shown in Figure 8. The sequence of welding (a total of 45 passes) is defined in the figure. The through-thickness path HAZo, as indicated in Figure 8, was selected for evaluation in this study.

The final residual stress distributions at 20 °C are shown in Figures 9 and 10 for the axial and hoop residual stress components, respectively. Note that the axial residual stress distribution in Figure 9 has a different shape to that seen in Figure 4 (case 1). This can be attributed the difference in geometry of the pipes. In this case the radius to thickness ratio of the pipe is smaller (2.8 versus 10.5), such that there exists a stronger mechanical constraint to suppress the 'tourniquet' deformation within the weld that led to high tensile stresses on the inner surface of the pipe in case 1.

The predicted residual stress distributions are compared for the isotropic, kinematic and mixed hardening models in Figures 11 and 12 against experimental measurements, taken from (Bate, 2000). The best agreement with experimental data is obtained for the isotropic hardening model, although good agreement is also obtained for the mixed hardening model. Both the predicted axial and hoop residual stresses correlate well with the measured data. In contrast to the isotropic and mixed hardening models, the stress magnitude was under estimated for the kinematic hardening model - a similar trend that was observed for case 1 (19mm thick pipe).

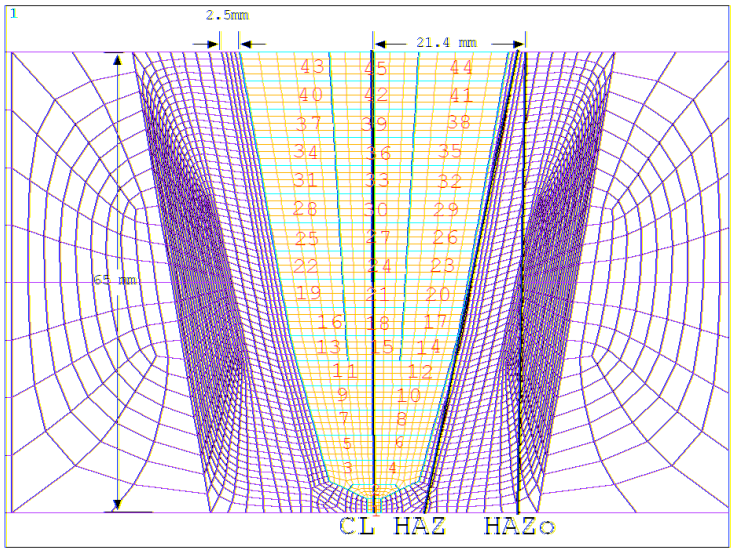

Figure 8: Geometry, finite element mesh and weld pass definition for Case 2.

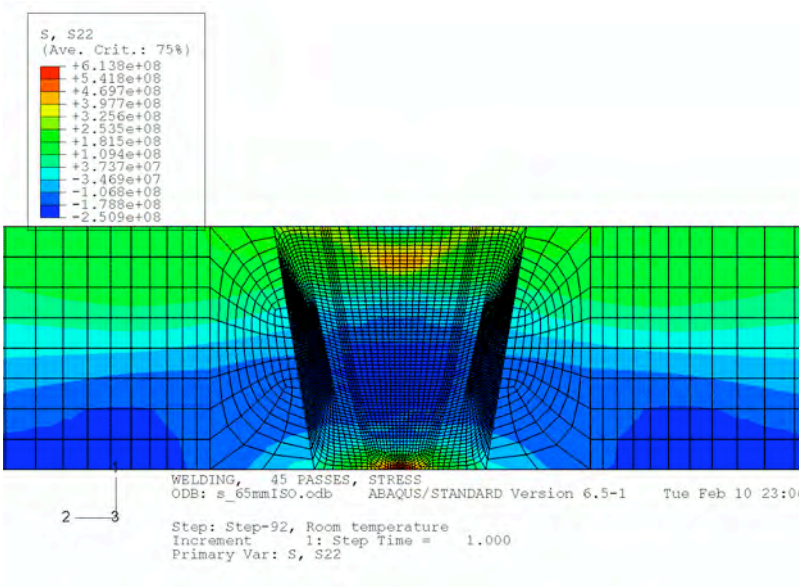

Figure 9: Axial residual stress for the thick-walled case 2 weld at 20 °C (unit Pa).

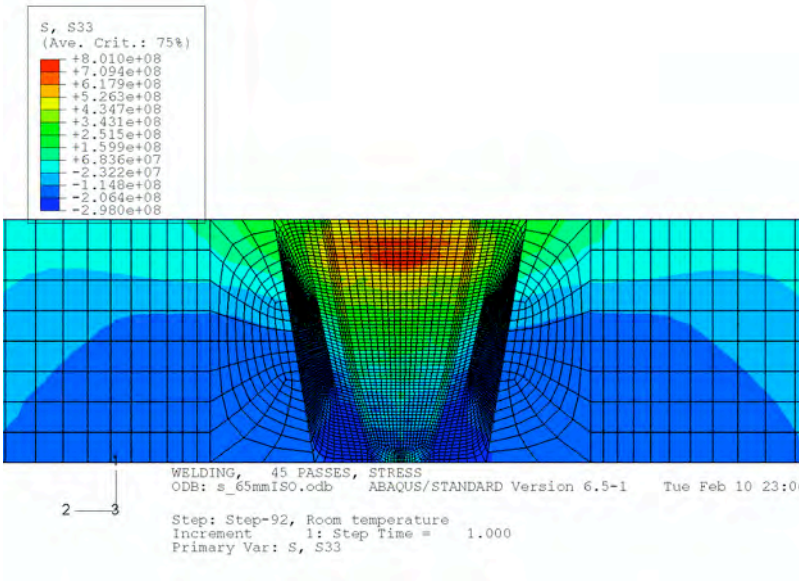

Figure 10: Hoop residual stress for the thick-walled case 2 weld at 20 °C (unit Pa).

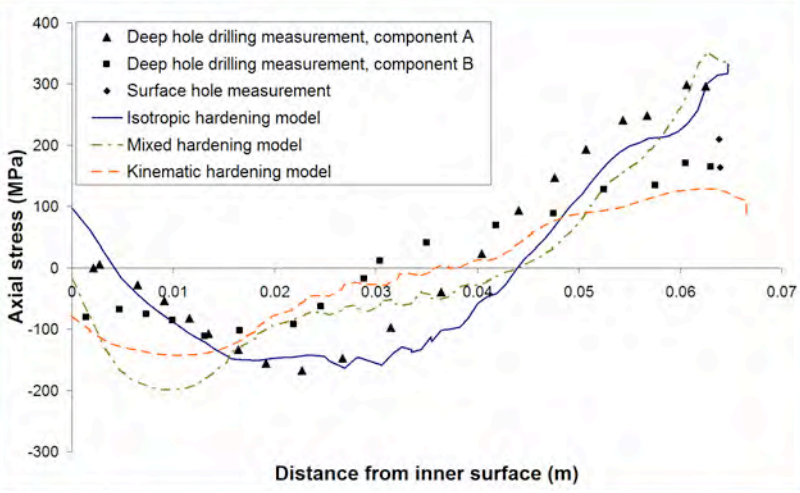

Figure 11: Case 2. Comparison of the predicted axial residual stress along path HAZo (defined in Figure 8) with the measured.

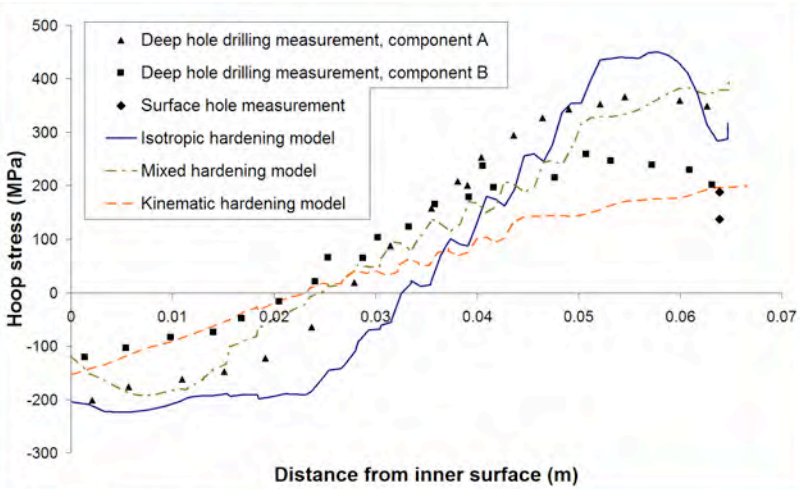

Figure 12: Case 2. Comparison of the predicted hoop residual stress along path HAZo (defined in Figure 8) with the measured.

6 DISCUSSION AND CONCLUSIONS

Stress fields were predicted from FE welding simulations using isotropic, kinematic and mixed hardening models and the distributions were compared with available experimental measurements. Two girth weld geometries were considered. The best predictions of the axial stress were obtained from the isotropic hardening model, regardless of geometry or measurement location. For the hoop stress the best predictions were obtained from the mixed hardening model, although the isotropic model also gave good agreement. In contrast the kinematic hardening model systematically under predicted the magnitude of the weld residual stress field for both the axial and the hoop stress. These trends were also observed along alternative paths, closer to the weld centreline, in a separate study by Mullins (2009).

The results indicate that an isotropic hardening model that is temperature sensitive and has fully defined strain hardening curves gives the best overall agreement with weld residual stress measurements. One instance in which the isotropic model did not give good agreement with experimental data was for the hoop stress for the 19mm thick weld (Case 1). In this case the hoop stress was underestimated on the inner surface of the pipe and overestimated on the outer surface. It is difficult to identify the cause of this discrepancy since for the 65mm thick weld (Case 2) good agreement for the hoop stress was obtained. The key difference between these welds is geometrical. In Case 1 the radius to wall thickness ratio is 10.5 whereas for Case 2 it is 2.8. It may be that 2D axisymmetric weld simulations with higher R_{in}/t ratios are overconstrained in the hoop direction due to the fact that the weld bead is effectively added instantaneously around the entire pipe circumference. Further investigation of this is required.

In those cases where the mixed hardening model gives better agreement, namely prediction of the hoop stress for the 19mm thick pipe, the isotropic model predictions tend to be excessively tensile. Assuming that fracture mechanical assessments based upon a critical crack size are of interest (not those based on the leak before break principle), it is advisable to use an isotropic hardening model in welding simulations - this appears to lead to conservative estimates of the residual stresses.

Acknowledgements. *We gratefully acknowledge funding from the Swedish Radiation Safety Authority (SSM) that allowed us to conduct this project.*

REFERENCES

Albertini, C. *et al*, "Dynamic Mechanical Properties of Austenitic Stainless Steels – Fitting of Experimental Data on Constitutive Equations," Proceedings of the 7th International Conference on Strutctural Mechanics in Reactor Technology, Division L, pp 53-62, 1983.

ASME SA-240, "Specification for heat-resisting chromium and chromium-nickel stainless steel plate, sheet and strip for pressure vessels", ASME, 2004.

Bate S.K., P.J. Bouchard, P.e.J. Flewitt, D. George, R.H. Leggatt and A.G. Youtsos, "Measurment and Modelling of Residual Stress in Thick Section Type 316 Stainless Steel Welds", Proc. Sixth International Conference on Residual Stresses, ICRS6, pp 1511-1518, Oxford University, Institute of Materials, UK, 2000.

Bouchard, P.J., "Validated residual stress profiles for fracture assessments of stainless steel pipe girth welds", Int. J. Pressure Vessels & Piping, Vol. 84, pp 195–222, 2007.

Bouchard, P.J., *et al*, "Measurement of the residual stresses in a stainless steel pipe girth weld containing long and short repairs," International Journal of Pressure Vessels and Piping, Vol 82, pp 299-310, 2005.

Dong, P. and Hong, J.K., "Fracture Mechanics Treatment of Residual Stresses in Defect Assessment", Welding in the World, Vol. 48, pp 28-38, 2004.

Dong, P., "Residual Stress Analysis of a Multi-Pass Girth Weld: 3D Special Shell Versus Axisymmetric Models," Journal of Pressure Vessel Technology, Vol. 123, p 207-213, 2001.

Edwards L, G. Bruno, M. Dutta, P.J. Bouchard, K.L. Abbott and R. Lin Peng, "Validation of Residual Stress Predictions for a 19 mm thick J-preparation Stainless Steel Pipe Girth Weld using Neutron Diffraction", Proc. Sixth International Conference on Residual Stresses, ICRS6, pp 1523-1526, Oxford University, Institute of Materials, UK, 2000.

Leggat, N. A., *et al*, "Numerical methods for welding simulation – the next technical step," Proceedings of 2008 ASME pressure vessels and piping division conference, PVP 2008-61498, 2008.

Lindgren, L., *et al*, "Dislocations, vacancies and solute diffusion in physical based plasticity model for AISI 316L", Mechanics of Materials, Vol 40, pp 907-919, 2008.

Mullins, J.G., Gunnars, J., "Influence of Hardening Model on Weld Residual Stress Distribution," Inspecta Technology Research Report No. 50002550-3, Rev 0, 2009.

Ogawa, K. *et al*, "The measurement and modelling of residual stresses in a stainless steel pipe girth weld," Proceedings of 2008 ASME pressure vessels and piping division conference, PVP 2008-61542, 2008.

Ohmi, Y. *et al*, "Constitutive modelling of proportional/nonproportional cyclic plasticity for type 316 stainless steel applicable to a wide temperature range," Materials Science Research International, Vol 1, No 4, pp 247-253, 1995.

Ohmi, Y. *et al*, "Formulation of constitutive models for cyclic deformation of type 316 stainless steel at high temperature," The Japan Society of Mechanical Engineers, No. 95-0074, pp 98-105, 1995.

Price J.W.H., Ziara-Paradowska A.M, Joshi S., Finlayson T., C Semetay C., Nied H., Comparison of experimental and theoretical residual stresses in welds: The issue of gauge volume, Int. J. Mechanical Sciences, Vol. 50, pp. 513-521, 2008.

Sandmeyer Steel Company, "Specs: 316, 316L & 317L", Sandmeyer Steel Company, 2009 (date accessed), http://www.sandmeyersteel.com/images/316-316L-317L-Spec-Sheet.pdf

Van Eeten, P.J.C., "Cyclic plasticity of a stainless steel: investigation of cyclic plasticity of 316L through experimental and numerical methods," Masters of Science Thesis, Department of Solid Mechanics, KTH University, Sweden, 2005.

Zang, W., Gunnars, J., "Improvement and validation of weld residual stress modelling procedure" Inspecta Technology Research Report No. 50002550-1, Rev 1, 2008.